

STRAIN AND WORK-HARDENING IN A COULOMB-TYPE  
GRANULAR MEDIUM

V. N. Nikolaevskii, N. M. Syrnikov,  
and M. É. Shaskol'skaya

Equations are given for the elastoplastic strain of a granular medium together with experimental relationships for sands. Equations for the characteristics are drawn up in general form for the two-dimensional case. It is shown that experimental data on the dilatancy rate as a function of the angle of internal friction reflect the condition for orthogonality of the characteristics of the velocity distribution to the direction of the dry-friction forces in the sliding areas. The flow in a shear tester is discussed. The calculation from the universal relationships agrees with experiment.

1. Equations

The following system of equations has been proposed [1, 2] to relate the increments in the elastic stresses  $de_{ij}^e$  and plastic ones  $de_{ij}^p$  to the state of strain:

$$\frac{de_{ij}}{dt} = \frac{1}{2} \left( \frac{\partial v_i}{\partial x_j} + \frac{\partial v_j}{\partial x_i} \right); \quad de_{ij} = de_{ij}^e + de_{ij}^p;$$

$$\frac{de_{ij}^e}{dt} = Q_{ijkl} \frac{\tilde{d}\sigma_{kl}}{dt};$$

$$Q_{ijkl} = \frac{1+\mu}{E} \delta_{ik} \delta_{jl} - \frac{\mu}{E} \delta_{ij} \delta_{kl};$$

$$de_{ij}^p = -(p+H) \delta_{ij} d\zeta + (\sigma_{ij} + p\delta_{ij}) d\lambda;$$

$$\Phi_\sigma(\sigma_{ij}, \alpha, H) = \frac{2}{\sqrt{3}} \kappa_\tau \tau - \alpha p - \alpha H = 0; \quad (1.1)$$

$$\Phi_\epsilon(de_{ij}^p, \Lambda) = de_p - \frac{2}{\sqrt{3}} \Lambda \kappa_\gamma d\gamma_p = 0, \quad (1.2)$$

where  $v_i$  is the rate of displacement,  $e_{ij}$  is the total strain,  $\mu$  is Poisson's ratio,  $E$  is Young's modulus,  $\sigma_{ij}$  is the stress tensor,  $d/dt$  is the symbol for the Jaumann derivative,  $p = -1/3 \sigma_{ij} \delta_{ij}$  is pressure,  $d\zeta$  and  $d\lambda$  are scalar functions differing from zero if the limiting conditions for the plastic state of (1.1) are met together with the dilatancy relation of (1.2),  $\alpha$  is the coefficient of internal friction,  $\alpha H$  is the adhesion,  $\Lambda$  is the dilatancy rate,  $\tau$  is the shear-stress intensity, and  $d\gamma^p$  is the plastic-shear intensity:

$$\tau^2 = \frac{1}{8} \{ (\sigma_{11} - \sigma_{22})^2 + (\sigma_{11} - \sigma_{33})^2 + (\sigma_{22} - \sigma_{33})^2 + 6(\sigma_{12}^2 + \sigma_{23}^2 + \sigma_{13}^2) \};$$

$$d\gamma_p^2 = \frac{1}{2} \{ (de_{11}^p - de_{22}^p)^2 + (de_{11}^p - de_{33}^p)^2 + (de_{22}^p - de_{33}^p)^2 + \\ + 6(de_{12}^p + de_{23}^p + de_{13}^p) \}; \quad \kappa_\tau = \text{sgn } \tau; \quad \kappa_\gamma = \text{sgn } d\gamma.$$

It can be seen that if we use (1.2) we can express  $d\zeta$  in terms of  $d\lambda$  and obtain the following form for the incremental plasticity law:

Moscow. Translated from Zhurnal Prikladnoi Mekhaniki i Tekhnicheskoi Fiziki, No. 3, pp. 181-190, May-June, 1975. Original article submitted April 1, 1974.

©1976 Plenum Publishing Corporation, 227 West 17th Street, New York, N.Y. 10011. No part of this publication may be reproduced, stored in a retrieval system, or transmitted, in any form or by any means, electronic, mechanical, photocopying, microfilming, recording or otherwise, without written permission of the publisher. A copy of this article is available from the publisher for \$15.00.

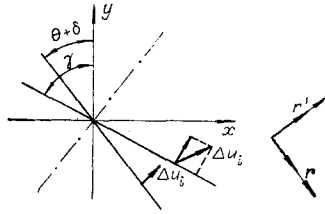


Fig. 1

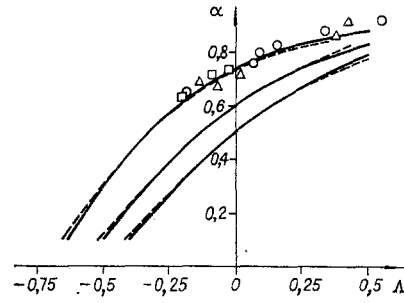


Fig. 2

$$de_{ij}^p = \left[ \sigma_{ij} + \frac{2}{3} \Lambda \alpha H \delta_{ij} + \left( 1 + \frac{2}{3} \Lambda \alpha \right) p \delta_{ij} \right] d\lambda, \quad (1.3)$$

where  $d\lambda \geq 0$  for  $\Phi_\sigma = 0$  and ongoing loading and  $d\lambda = 0$  if there is unloading ( $\Phi_\sigma < 0$ ) or  $\Phi_\sigma = 0$  but the loading is neutral. Relation (1.3) becomes the flow law, and (1.1) becomes the associative Mises-condition for  $\Lambda \equiv \alpha$ ; in the general case, with  $\Lambda \neq \alpha$ , (1.3) corresponds to a nonassociative incremental law.

We will assume that  $\alpha$  and  $\Lambda$  are functions of the state parameter  $\chi$ ; we assume that  $\chi = e_p / e_p^*$ , where  $e_p^*$  is strain such that the medium does not dilate (is in the critical state  $\Lambda(\chi = 1) = 0$ ); also  $e_p^* = f(p)$  is some function of pressure. Since  $\alpha = \alpha(\chi)$  and  $\Lambda = \Lambda(\chi)$  are functions of the same parameter, we can use also hardening functions of the form  $\alpha = \alpha(\chi)$ ,  $\Lambda = \Lambda(\alpha)$ .

## 2. Planar Plastic Deformation

This particular case is characterized by the position  $de_{33}^p = de_{13}^p = de_{23}^p = 0$ ; then we have that (1.1) and (1.2) become

$$\sqrt{\frac{1}{4} (\sigma_x - \sigma_y)^2 + \sigma_{xy}^2} + \frac{1}{2} (\sigma_x + \sigma_y) \sin \varphi - H \sin \varphi = 0, \quad (2.1)$$

where  $\varphi$  is the angle of internal friction, with

$$\sin \varphi = \alpha \frac{\sqrt{3(3 - \Lambda^2)}}{3 - \alpha \Lambda}; \quad (2.2)$$

$$de_x^p + de_y^p - \sin \nu \sqrt{(de_x^p - de_y^p)^2 + 4de_{xy}^2} = 0, \quad (2.3)$$

where  $\nu$  is the dilatancy angle, with

$$\sin \nu = \Lambda \sqrt{\frac{3}{3 - \Lambda^2}}. \quad (2.4)$$

The incremental plastic-strain law now has the form

$$de_{ij}^p = \left[ \sigma_{ij} + \sin \varphi \sin \nu H \delta_{ij} - \left( 1 + \sin \varphi \sin \nu \right) \frac{1}{2} \sigma_{ij} \delta_{ij} \right] d\lambda, \quad (2.5)$$

where  $i, j = x, y$ .

If we now neglect the elastic components of the strains, i.e., assume  $de_{ij}^e \equiv 0$ , we get a model for a rigid-plastic dilating material [3], and then

$$de_x = \frac{\partial u}{\partial x} dt; \quad de_y = \frac{\partial v}{\partial y} dt; \quad de_{xy} = \frac{1}{2} \left( \frac{\partial u}{\partial y} + \frac{\partial v}{\partial x} \right) dt.$$

The equilibrium conditions for the two-dimensional case include three unknowns:

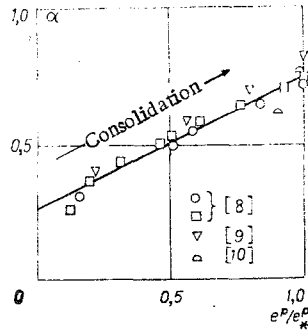


Fig. 3

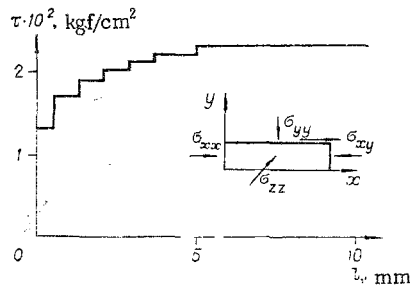


Fig. 4

$$\frac{\partial \sigma_x}{\partial x} + \frac{\partial \sigma_{xy}}{\partial y} = F_x, \quad \frac{\partial \sigma_{xy}}{\partial x} + \frac{\partial \sigma_y}{\partial y} = F_y \quad (2.6)$$

for given mass forces  $F_x$  and  $F_y$ ; the standard substitution

$$\begin{aligned} \sigma_x &= -p + (p+H) \sin \varphi \cos 2\theta; & \sigma_y &= -p - (p+H) \sin \varphi \cos 2\theta; \\ \sigma_{xy} &= - (p+H) \sin \varphi \sin 2\theta, \end{aligned} \quad (2.7)$$

with  $\theta$  the inclination of the maximal principal compressive stress  $\sigma_2$  to the  $y$  axis (or, which is the same, of the principal stress  $\sigma_1$  to the  $x$  axis), enables us to satisfy condition (2.1) identically and to convert (2.6) to the form

$$\begin{aligned} \frac{\partial p}{\partial x} (1 - \psi'_p \cos 2\theta) + \frac{\partial p}{\partial y} \psi'_p \sin 2\theta - \psi'_p \cos 2\theta \frac{\partial \rho}{\partial x} + \\ + \psi'_p \sin 2\theta \frac{\partial \rho}{\partial y} - 2\psi \sin 2\theta \frac{\partial \theta}{\partial x} - 2\psi \cos 2\theta \frac{\partial \theta}{\partial y} = -F_x; \end{aligned} \quad (2.8)$$

$$\begin{aligned} \frac{\partial p}{\partial x} \psi'_p \sin \alpha + (1 + \cos 2\theta \psi'_p) \frac{\partial p}{\partial y} + \sin 2\theta - \psi'_p \frac{\partial \rho}{\partial x} + \\ \frac{\partial \rho}{\partial y} \cos 2\theta \psi'_p + 2\psi \cos 2\theta \frac{\partial \theta}{\partial x} - 2\psi \sin 2\theta \frac{\partial \theta}{\partial y} = -F_y, \end{aligned} \quad (2.9)$$

where  $\psi = (p+H) \sin \varphi$ ;  $\psi'_p$  and  $\psi'_\rho$  are the corresponding partial derivatives.

To get the equation for the distribution of the velocities  $u$  and  $v$  we substitute (2.7) into (2.5), whereupon obvious steps give

$$\begin{aligned} \sin 2\theta \frac{\partial u}{\partial x} + \cos 2\theta \frac{\partial u}{\partial y} + \cos 2\theta \frac{\partial v}{\partial x} - \sin 2\theta \frac{\partial v}{\partial y} = 0; \\ \sin 2\theta \frac{\partial u}{\partial x} + \sin \nu \frac{\partial u}{\partial y} + \sin \nu \frac{\partial v}{\partial x} + \sin 2\theta \frac{\partial v}{\partial y} = 0. \end{aligned} \quad (2.10)$$

If we eliminate  $\partial u/\partial y + \partial u/\partial x$  from (2.10), we at once get (2.3) expressed in terms of the maximal shear rate for an arbitrary [4] coordination system:

$$\frac{\partial u}{\partial x} + \frac{\partial v}{\partial y} = \frac{\sin \nu}{\cos 2\theta} \left( \frac{\partial u}{\partial x} - \frac{\partial v}{\partial y} \right).$$

As  $\varphi = \varphi(\rho, p)$  and  $\nu = \nu(\rho, p)$ , the system of equations for two-dimensional motion of (2.8) and (2.10) should be supplemented with the equation of continuity:

$$\frac{\partial \rho}{\partial t} + u \frac{\partial \rho}{\partial x} + v \frac{\partial \rho}{\partial y} + \rho \frac{\partial u}{\partial x} + \rho \frac{\partial v}{\partial y} = 0.$$

### 3. Equations for the Characteristics in the Two-Dimensional Case

It can be shown that the equations for the characteristics for the stress distribution take the following form:

$$\left(\frac{dy}{dx}\right)_{1,2} = \frac{\sin 2\theta \pm \sqrt{1 - \psi_p'^2}}{-\cos 2\theta + \psi_p'} = \operatorname{ctg}(\theta \pm \varepsilon), \quad (3.1)$$

where  $\psi_p' = \cos 2\varepsilon$  and  $|\psi_p'| \leq 1$ ; if  $\psi_p = \sin \varphi$ , as in classical statics [5], then  $\varepsilon = \pi/4 - \varphi/2$ .

The equations for the characteristics of the velocity distribution take the form

$$\frac{dy}{dx} = \frac{-\sin 2\theta \pm \sqrt{1 - \cos^2 2\delta}}{\cos 2\delta - \cos 2\theta} = \frac{\sin 2\theta \pm \sqrt{1 - \cos^2 2\delta}}{\cos 2\theta - \cos 2\delta} = \operatorname{ctg}(\theta \pm \delta), \quad (3.2)$$

where  $\sin \nu = \cos 2\delta$ , i.e.  $\delta = \pi/4 - \nu/2$ . Finally, the fifth characteristic, for the density, for  $\partial\rho/\partial t \equiv 0$  coincides with the particle path:

$$\left(\frac{dy}{dx}\right)_5 = \frac{v}{u}. \quad (3.3)$$

The conditions on the characteristics may be represented in the following general form:

$$\begin{aligned} & [dx^2(\cos 2\theta - \cos 2\delta) - dy^2(\cos 2\theta + \cos 2\delta) + \\ & + 2\sin 2\theta dx dy] \{dp(v dx - u dy) [dx(-\cos 2\theta - \cos 2\varepsilon) + \\ & + \sin 2\theta dy] + \psi_p' d\rho dy (u dx + v dy) - d\theta dy \psi (v dx - u dy)\} - \\ & - 2\rho dy \cos 2\delta (dudx + dvdy) (dx^2 + dy^2) \psi \psi_p' = 0. \end{aligned} \quad (3.4)$$

To obtain the conditions along a particular characteristic from (3.4) we need to substitute for the corresponding value of  $dy/dx$  from (3.1)-(3.3).

For instance, for the velocity characteristic we have

$$\begin{aligned} \frac{\partial u}{\partial s_3} + \operatorname{ctg}(\theta + \delta) \frac{\partial v}{\partial s_3} &= 0, \\ \frac{\partial u}{\partial s_4} + \operatorname{ctg}(\theta - \delta) \frac{\partial v}{\partial s_4} &= 0. \end{aligned} \quad (3.5)$$

The same conditions written in terms of the projections of the velocity on the direction of the characteristic have been given in [4]:

$$\begin{aligned} \frac{\partial U}{\partial s_3} - (V \operatorname{cosec} 2\delta - U \operatorname{ctg} 2\delta) \frac{\partial(\theta - \delta)}{\partial s_3} &= 0; \\ \frac{\partial V}{\partial s_4} + (U \operatorname{cosec} 2\delta - V \operatorname{tg} 2\delta) \frac{\partial(\theta + \delta)}{\partial s_4} &= 0. \end{aligned}$$

The conditions obeyed along the density characteristic take the following form:

$$(\cos 2\theta + \cos 2\delta) \left[ \frac{v}{u} + \operatorname{tg}(\theta + \delta) \right] \left[ \frac{v}{u} + \operatorname{tg}(\theta - \delta) \right] d\rho - \rho \cos 2\delta d(u^2 + v^2) = 0.$$

These relationships for the characteristics generalize the results of [4] to a body showing work hardening.

Finally, in the hypothetical case  $\nu = \varphi$  the results correspond to the conditions for associative flow, while for  $\nu = \varphi, = \text{const}$  they coincide with Shield's results [6].

#### 4. Derivation of the Hardening Functions

When we have found  $\varphi = \varphi(\rho, p)$  and shield,  $\nu = \nu(\rho, p)$ , we convert to the general three-dimensional case to find the above work-hardening functions  $\alpha(\chi)$  and  $\Lambda = \Lambda(\alpha)$ .

Consider the relative motion in an elementary volume of the medium represented by a strain rate  $e_{ij}$ ; the velocity of the relative displacements of two particles in the medium lying on unit section  $r$  (Fig.

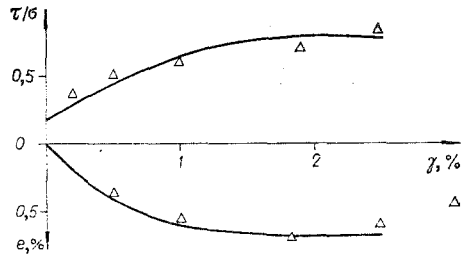


Fig. 5

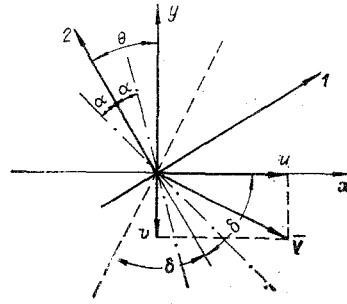


Fig. 6

1) is expressed in terms of the tensor  $e_{ij}$  in an arbitrary\* coordinate system  $x$  and  $y$  as follows:

$$\Delta u_i = e_{ij} r_j, \quad r(\sin \gamma, -\cos \gamma),$$

where  $\gamma$  is the angle between the line joining the centers of the particles and the  $y$  axis. The projection of the vector  $\Delta u_i$  on the direction of  $r$  and on the direction perpendicular to it  $r'(\cos \gamma, \sin \gamma)$  will be

$$\Delta u_i r_i = \frac{\partial u}{\partial x} \sin^2 \gamma - \left( \frac{\partial u}{\partial y} + \frac{\partial v}{\partial x} \right) \sin \gamma \cos \gamma + \frac{\partial v}{\partial y} \cos^2 \gamma; \quad (4.1)$$

$$\Delta u_i r'_i = \frac{1}{2} \left\{ \left( \frac{\partial u}{\partial x} - \frac{\partial v}{\partial y} \right) \sin 2\gamma - \left( \frac{\partial u}{\partial y} + \frac{\partial v}{\partial x} \right) \cos 2\gamma \right\}.$$

Equation (4.1) will simulate the microscopic motions in a granular medium (a system of hard spheres, on a system of disks in the two-dimensional case) if, firstly, the velocity gradients satisfy (2.9) and, secondly, if there is scope for relative slip of the adjacent particles. We find that

$$\Delta u_i r_i = 0; \quad \Delta u_i r'_i = A \sin 2(\theta \pm \delta) \neq 0$$

for  $\gamma = \theta \pm \delta$ , i.e., when the direction of  $\bar{r}$  coincides with the characteristic velocity distribution and the velocity vector  $\Delta u$  is orthogonal to the characteristic for the velocity distribution. In all other cases,  $\gamma \neq \theta \pm \delta$ , and the component of the relative velocity  $\Delta u_i$  along  $\bar{r}$  will be different from zero. Then the purely tangential relative motion of the particles such that the relative velocity is orthogonal to a line joining the centers of adjacent particles occurs along a family of lines mutually orthogonal to the families of characteristics for the velocity distribution. It has been pointed out [4] that it is precisely these lines that should be interpreted as the slip lines. The characteristics of the velocity distribution will simultaneously be slip lines only for an incompressible medium ( $\nu = 0$ ).

The microscopic motion in a Coulomb medium occurs with dry-friction forces acting along the slip lines. It has been supposed [4] that the dry-friction force  $R$  acting on the limiting-equilibrium area at an angle  $\beta$  is collinear with the direction of the slip line (i.e., is orthogonal to one of the characteristics of the velocity distribution). Then the following relation applies between the internal-friction angles and the dilatancy in the two-dimensional case:

$$\varphi = 2 \left( \frac{\pi}{4} - \delta + \varphi_0 \right) = 2\varphi_0 + \nu, \quad (4.2)$$

where  $\varphi_0$  can be interpreted as the angle of friction between two individual particles.

Equation (4.2) can be converted to the general case of a relation between the work-hardening functions  $\alpha$  and  $\Lambda$ , which are dependent on the parameter  $\chi = e^D / e^D_*$ ; we substitute (4.2) into (2.2) and eliminate  $\nu$  and use (2.4) to get  $\alpha(\Lambda)$ ; the resultant  $\varphi_0 = 15, 18.5, 23^\circ$  curves are shown in Fig. 2 for three values of the parameter; these relationships are represented with reasonable accuracy (broken lines) by the formula

$$\Lambda = b - \sqrt{1 + 2b\alpha_*} - (\alpha_* + 2b)\alpha, \quad (4.3)$$

$$b = \sqrt{1 - \alpha_*},$$

\*In the particular case where the axes of  $x$  and  $y$  coincide with the principal axes of the strain-rate tensor, an analogous analysis has already been given in [4].

where  $\alpha_* = \alpha(\Lambda = 0) = \sin 2\varphi_0$ .

We now compare these relationships with the listed experimental data [7] of the coefficient of internal friction as a function of the dilatancy rate, as measured during triaxial tests on various river sands. (In [7] the experimental data are represented as  $\varphi = \arcsin[(\sigma_1 - \sigma_2)/(\sigma_1 + \sigma_2)]$ , as a function of  $de_v/de_1$ , which is called there the dilatancy rate, where  $e_1$  and  $e_v$  are the axial and volume deformations, while  $\sigma_1$  and  $\sigma_2$  are the axial and lateral stresses). Figure 2 shows the results of conversion to the functions used here. The data for the various sands (various symbols), are closely approximated by the single relationship of (4.3) with  $\varphi_0 = 23^\circ$ . This value of  $\varphi_0$  also correlates satisfactorily with the data of the angle of friction between two quartz surfaces:  $17-26^\circ$ .

The second relationship  $\alpha(\chi)$  can be found by processing the experimental data on triaxial tests on river sands [8-11]. It is found that over a considerable range  $\alpha(\chi)$  can be described by a single linear relationship of the following form (Fig. 3):

$$\alpha = \alpha_0 + (\alpha_* - \alpha_0)\chi, \quad (4.4)$$

where  $\alpha_0 = \alpha(0)$  and  $\alpha_* = \alpha(1)$ ; note that  $\chi = 1$  corresponds to the critical value for bulk plastic deformation  $e^p = e_*^p$ , at which  $\Lambda$  becomes zero.

### 5. Two-Dimensional Shear

Equations (4.3) and (4.4) have been used in [11] to perform calculations on one-dimensional axially symmetrical limiting states, and the results agreed satisfactorily with triaxial tests. Here we consider a planar section of a granular medium, which corresponds to tests on simple-shear equipment in measurements on the internal friction due to adhesion.

In practice, the shear strain in such tests varies in a stepwise fashion as the shear stresses  $\sigma_{xy}$  increase (Fig. 4) up to some critical value  $\sigma_{xy}^*$  (the stress  $\sigma_{yy} = \text{const}$ ), where the shear strain begins to increase without limit (failure).

We now formulate the definitive equations for this case and note that the elastic components of the strains can be neglected, since the stresses in tests on sands in such equipment are usually low ( $\sigma_{yy} = 3-4 \cdot 10^{-3} \text{ kg/cm}^2$  [12]).

In the present case  $de_{xx} = de_{zz} = de_{xz} = de_{yz} = 0$ ;  $de_{ij} = de_{ij}^p$ ;  $de = de_{yy}$ ;  $de_{xy} = d\gamma$  and the general relations of (1.3) take the form

$$\begin{aligned} de &= \left[ \sigma + \left( 1 + \frac{2\Lambda\alpha}{3} \right) p \right] d\lambda; & d\gamma &= \tau d\lambda; \\ \sigma &= \sigma_{yy}; & \tau &= \sigma_{xy}; \\ p &= -1/3(\sigma_{xx} + \sigma_{yy} + \sigma_{zz}), \end{aligned} \quad (5.1)$$

with

$$\begin{aligned} \frac{\sigma_{xx}}{\sigma} = \frac{\sigma_{zz}}{\sigma} &= \frac{3 + 2\alpha\Lambda}{3 - 4\alpha\Lambda} = L(e); \\ \sigma_{xz} = \sigma_{yz} &= 0. \end{aligned} \quad (5.2)$$

The flow condition of (1.1) may be put as

$$\frac{\tau}{\sigma} = -\frac{1}{3} \{ \alpha^2 (1 + 2L(e))^2 - 3(1 - L(e))^2 \}^{1/2} = -k(e). \quad (5.3)$$

We eliminate  $d\lambda$  from (5.1) to get an ordinary differential equation relating the bulk and shear deformations:

$$\frac{de}{d\gamma} = -\frac{1}{k(e)} \{ 1 - (3 + 2\alpha\Lambda)(1 + 2L/9) \}.$$

If this nonlinear equation is integrated, we can find the function  $e = e(\gamma)$  and then calculate the ratio  $k = \tau/\sigma$  as a function of the shear strain  $e_{xy}$ ; Fig. 5 shows results from numerical integration, and also the experimental data of [12]. The critical bulk strain  $e_*^p$  was selected from the data of [12] as 0.7%. The calculation is in satisfactory agreement with experiment. Here we took from experiment only one param-

eter  $e_*^D$  and the agreement of theory with experiment again indicates that the model can be used to describe the behavior of a granulated medium under various conditions.

It follows from (5.3) that  $L=1$  and  $k = \alpha_*$  only if  $e = e_*^D$ ; the parameter  $k = |\tau^*/\sigma|$  is measured in experiments on two-dimensional shear and is interpreted as  $\tan \varphi_p$ , where  $\varphi_p$  is the internal-friction angle measured for sand in this way in the planar case. As  $\alpha_*$  was taken as 0.72-0.76 in the model, the critical value  $\varphi_p^*$  measured with a simple shear apparatus should be 36-38°, which also agrees with experiment [7, 12]. In this connection we note that the critical value for the internal-friction angle measured in a standard triaxial test as  $\varphi_t = \arcsin(\sigma_1 - \sigma_2)/(\sigma_1 + \sigma_2)$  differs from  $\varphi_p^*$  for the same sand and is 30-32° [7], and corresponds to the value of the parameter  $\alpha_* = 0.72 - 0.76$ , with  $\sigma_1$  the axial stress in the above and  $\sigma_2 = \sigma_3$  the lateral stress. Finally, the critical effective internal-friction angle  $\varphi_*$  introduced in [4] is equal to  $\arcsin \alpha_*$  and about 46°, since it determines the position of the areas of limiting equilibrium with respect to the principal axes (these areas do not coincide with the plane of shear).

We consider in more detail the characteristics of the stress and velocity distributions in planar shear. The positions of the principal axes of the shears and strain rates are defined by the angle  $\theta$ :

$$\operatorname{tg} 2\theta = \frac{2\sigma_{xy}}{\sigma_{xx} - \sigma_{yy}}.$$

We substitute here for the stress components in accordance with (5.2) and (5.3) and use  $\nu = \Lambda \sqrt{3(3 - \Lambda^2)}$  to get

$$2\psi = \arccos \left( -\frac{\Lambda \sqrt{3}}{\sqrt{3 - \Lambda^2}} \right) = \frac{\pi}{2} + \nu = \pi - 2, \quad \psi = \frac{\pi}{2} - \delta.$$

Consequently, the angle between the x axis and the direction of maximum principal compressive strength is  $\delta$  (Fig. 6), and the x axis is the characteristic of the velocity distribution. The same result can be obtained directly from the fact that

$$\frac{de_{xx}}{dt} = \frac{du}{dx} = 0.$$

The second characteristic is [4] orthogonal to the velocity vector  $\mathbf{V}$ , which is directed along the line of the relative slip of the particles. When the bulk strain reaches the critical value  $e_*^D$  the dilatancy rate  $\Lambda$  and  $\mathbf{V}$  is directed along the x axis, i.e., the slip direction coincides with the characteristic of the velocity distribution; there is unrestricted shear in the direction of the x axis without change of volume. The angle between the x axis and the principal axis 2 in that case is  $\pi/4$ .

There is [1] a linear velocity distribution for each instant in the sheared layer,

$$u = \frac{U}{h} y; \quad v = \frac{U}{h} y \operatorname{tg} \nu, \quad (5.4)$$

that satisfies (2.3); the relations of (3.5) along the characteristics give us that along the first characteristic for planar shear we have  $u = U = \text{const}$ , while along the second we have  $\mathbf{V} \equiv 0$ .

The dot-dashed lines in Fig. 6 show the positions of the limiting-equilibrium areas, which form the angles  $\pi/4 - \varphi/2$  with the direction of the axis of the maximum principal compressive stress. Condition (2.1) is met by these areas with an effective internal-friction angle  $\varphi$  defined by (2.2). These areas in real cases with  $\varphi \neq 0$  do not coincide with the slip direction, while for  $\Lambda = 0$  the angle between the x axis and a limiting-equilibrium area is  $\varphi_0$ , i.e., about 23°.

Equations (2.7) for the components of the stress tensor in this case take the form

$$\left. \begin{matrix} \sigma_{xx} \\ \sigma_{yy} \end{matrix} \right\} = -p(1 \pm \sin \varphi \sin \nu); \quad \sigma_{xy} = p \sin \varphi \cos \nu,$$

and therefore

$$k = \frac{\tau}{\sigma} = \frac{\cos \nu \cdot \sin \varphi}{1 - \sin \nu \cdot \sin \varphi}. \quad (5.5)$$

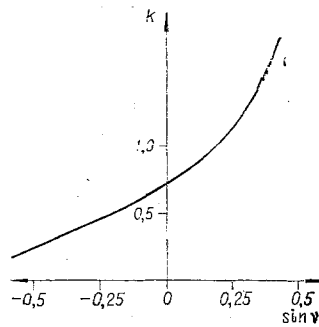


Fig. 7

Equation (5.5) may be derived [1] directly from the velocity distribution of (5.4) for the thickness of the layer; as  $\varphi$  is given by (4.2) as a function of  $\nu$ , one can say that we have a  $k(\nu)$  relation for this flow. This relationship is shown in Fig. 7 for  $\varphi_0 = 23^\circ$  (the relationship was given in [1] for  $\varphi_0 = 30^\circ$ ).

If, on the other hand, we interpret the data on planar shear via the model for a Coulomb incompressible medium, then  $k = \operatorname{tg} \varphi_p$ , and the graph (Fig. 7) might be treated as evidence of an effective  $\varphi_p = \varphi_p(e)$  relationship, but the displacement recorded in the experiments (measurements of the kinematic variables) remain inexplicable. This is why the dilatancy effect is of particular significance when there are displacements specified at the boundaries, as in calculating the forces acting on a rotating supported well [13].

Experimental data of the type shown in Figs. 4 and 5 have been explained qualitatively [14] via a model for a plastic body with an associative flow law and modal points on the flow surface.

#### LITERATURE CITED

1. V. N. Nikolaevskii, "Mechanical properties of soils and the theory of plasticity," in: Surveys of Science and Technology, Series: Mechanics of Deformable Solids [in Russian], Vol. 6, VINTI, Moscow (1972).
2. V. N. Nikolaevskii, "Continuum theory of plastic deformation of a granular medium," in: Foundations of Plasticity (edited by A. Sawczuk), Noordhoff, Llyden (1972).
3. V. N. Nikolaevskii, "The definitive equations of plastic flow for granular media," Prikl. Mat. Mekh. 35, No. 6 (1971).
4. V. N. Nikolaevskii and N. M. Syrnikov, "The planar limiting flow of a granular dilating medium," Izv. Akad. Nauk SSSR, Mekh. Tverd. Tela, No. 2 (1970).
5. V. V. Sokolovskii, Statics of a Granular Medium [in Russian], Fizmatgiz, Moscow (1960).
6. R. T. Shield, "Mixed boundary value problems in soil mechanics," Quart. J. Appl. Math., 11, No. 1 (1953).
7. A. W. Bishop, "The strength of soils as engineering materials," Geotechnique, 16, No. 2 (1966).
8. A. S. Vesic and G. W. Clough, "Behavior of granular materials under high stresses," J. Soil Mech. Found. Div. Proc. Amer. Soc. Civ. Eng., 94, No. 3 (1968).
9. L. Barden, H. Ismail, and P. Tong., "Plane strain deformation of granular material at low and high pressures," Geotechnique, 19, No. 4 (1969).
10. S. Fridman and T. G. Zeitlen, "Some pseudo-elastic properties of granular media," in: Proceedings of the Seventh International Conference on Soil Mechanics and Foundations of Engineering, Mexico, Vol. 1 (1969).
11. V. N. Nikolaevskii, N. M. Syrnikov, and G. M. Shefter, "Dynamics of elastoplastic dilating media," in: Advances and Attainments of Mechanics of Deformable Solids [in Russian], Moscow (1974).
12. V. V. Adushkin and T. A. Orlenko, "Strength characteristics and consolidation of sandy soil under shear," Izv. Akad. Nauk SSSR, Mekh. Tverd. Tela, No. 2 (1970).
13. K. H. Roscoe, "The influence of strain in soil mechanics," Geotechnique, 20, No. 2 (1970).
14. D. D. Ivlev and G. I. Bykovtsev, Theory of Work-Hardening Plastic Solids [in Russian], Nauka, Moscow (1971.)